Single-Molecule FRET Studies of Counterion Effects on the Free Energy Landscape of Human Mitochondrial Lysine tRNA

ARTICLE *in* BIOCHEMISTRY · MARCH 2011

Impact Factor: 3.02 · DOI: 10.1021/bi101804t · Source: PubMed

5 AUTHORS, INCLUDING:

Martin Hengesbach
Goethe-Universität Frankfurt am Main
20 PUBLICATIONS **148** CITATIONS
SEE PROFILE

Mark Helm
Johannes Gutenberg-Universität Mainz
113 PUBLICATIONS **2,739** CITATIONS
SEE PROFILE

Andrei Yu Kobitski
Karlsruhe Institute of Technology
54 PUBLICATIONS **935** CITATIONS
SEE PROFILE

BIOCHEMISTRY
including biophysical chemistry & molecular biology

ARTICLE

pubs.acs.org/biochemistry

Single-Molecule FRET Studies of Counterion Effects on the Free Energy Landscape of Human Mitochondrial Lysine tRNA

Kirsten Dammertz,[†,#] Martin Hengesbach,[‡,&] Mark Helm,[‡,§] G. Ulrich Nienhaus,[∥,⊥] and Andrei Yu. Kobitski*[,∥]

[†]Institute of Biophysics, University of Ulm, 89069 Ulm, Germany

[‡]Institute of Pharmacy and Molecular Biotechnology, Heidelberg University, 69120 Heidelberg, Germany

[§]Institute of Pharmacy and Biochemistry, University of Mainz, 55128 Mainz, Germany

[∥]Institute of Applied Physics and Center for Functional Nanostructures (CFN), Karlsruhe Institute of Technology (KIT), 76128 Karlsruhe, Germany

[⊥]Department of Physics, University of Illinois at Urbana−Champaign, Urbana, Illinois 61801, United States

Supporting Information

ABSTRACT: The folding energy landscape of RNA is greatly affected by interactions between the RNA and counterions that neutralize the backbone negative charges and may also participate in tertiary contacts. Valence, size, coordination number, and electron shell structure can all contribute to the energetic stabilization of specific RNA conformations. Using single-molecule fluorescence resonance energy transfer (smFRET), we have examined the folding properties of the RNA transcript of human mitochondrial $tRNA^{Lys}$, which possesses two different folded states in addition to the unfolded one under conditions of thermodynamic equilibrium. We have quantitatively analyzed the degree of RNA tertiary structure stabilization for different types of cations based on a thermodynamic model that accounts for multiple conformational states and RNA−ion interactions within each state. We have observed that small monovalent ions stabilize the tRNA tertiary structure more efficiently than larger ones. More ions were found in close vicinity of compact RNA structures, independent of the type of ion. The largest conformation-dependent binding specificity of ions of the same charge was found for divalent ions, for which the ionic radii and coordination properties were responsible for shaping the folding free energy.

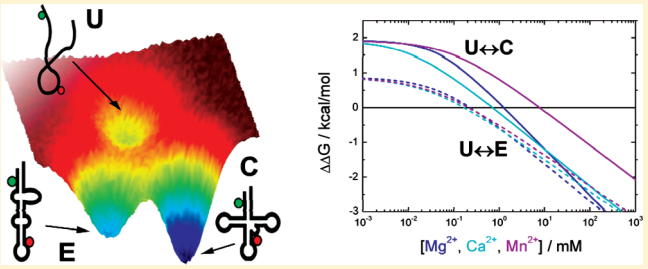

The presence of positively charged counterions is crucial for the folding of polyanionic RNA molecules.[1,2] Mono- and divalent cations such as Na^+, K^+, and Mg^{2+} are very effective at screening the RNA backbone negative charge. Divalent ions may also be completely or partially coordinated by RNA at specific binding sites and can, therefore, be essential factors for the formation of the proper RNA tertiary structure.[3] Mg^{2+} ions are especially important for the formation of complicated structural features such as binding pockets and catalytic centers. Divalent cations may also play crucial roles in the catalytic action of ribozymes.[4,5] The more effective stabilization of tertiary structure by some ions over others was recognized several decades ago,[6−8] but quantitative thermodynamic descriptions of RNA−ion interactions were attempted only recently.[9−17]

RNA folding typically includes a transition from an unfolded state in the absence of ions to a counterion-mediated intermediate state that chiefly consists of elements of secondary structure such as locally stable hairpin, bulge, and loop motifs. A second transition to a collapsed folded state with multiple tertiary contacts typically requires the presence of divalent cations.[3] The concept of a funnel-shaped energy landscape (Figure 1A) guiding the molecules toward a multitude of folded states, which was originally introduced for proteins,[18,19] has also been applied to RNAs.[20] However, unlike proteins, RNA forms very stable secondary structure elements, giving rise to highly rugged energy landscapes with deep local minima that correspond to misfolded conformations.[21−23] Conformational transitions involving such metastable states are strongly affected by cations, especially multivalent cations.[24] Therefore, a thorough understanding of the RNA conformational landscape requires a detailed investigation of the structural, dynamic, and energetic aspects of folding, with special emphasis on the effect of polyvalent cations.

Among RNAs with well-defined three-dimensional structures, tRNA is arguably among the best-studied examples. Its canonical three-dimensional "L" shape is based on a secondary structure arrangement in the form of a cloverleaf. Typically, tRNAs

Received: November 10, 2010
Revised: March 4, 2011
Published: March 07, 2011

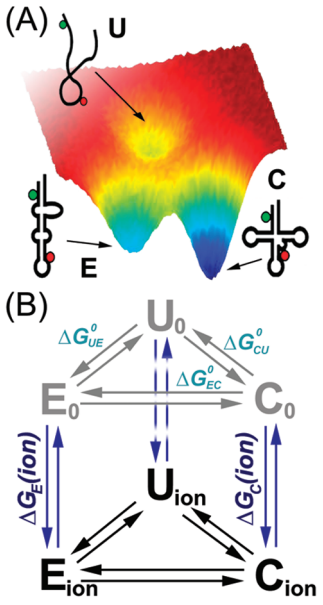

Figure 1. (A) Schematic depiction of the free energy landscape of unmodified (Kwt) $tRNA^{Lys}$, with unfolded (**U**), extended hairpin (**E**), and cloverleaf-based L-shape (**C**) conformations. (B) Thermodynamic scheme describing the equilibrium between the ion-free and ion-bound states within the **U**, **E**, and **C** conformations.

spontaneously fold into their functional conformation right after transcription. A notable exception to this rule is human mitochondrial lysine tRNA (mt $tRNA^{Lys}$), which requires multiple post-transcriptional modifications for proper folding under physiological conditions.[25−27] It carries altogether six modifications; one of them, methylation of *N1* of adenosine 9 (m^1A9), is known to strongly affect the relative free energies of three structurally distinct conformations (Figure 1A and Figure S1)—the unfolded (**U**), extended hairpin (**E**), and cloverleaf-based L-shape (**C**) states—the structural properties of which have been thoroughly discussed.[15] The changing fractions of multiple subpopulations at different ion concentrations complicate a quantitative analysis on the ensemble level. By contrast, single-molecule fluorescence experiments, which can distinguish between these states, may afford unprecedented insights into the structure and dynamics of biopolymers including RNA.[28] For human mt $tRNA^{Lys}$, single-molecule fluorescence (Förster) resonance energy transfer (smFRET) measurements allowed the separation of structural contributions (i.e., base modifications) and RNA−ion interactions to the energetics of each individual conformational state.[15]

The binding of ions to RNA may occur either as a nonspecific accumulation of a diffuse counterion cloud or as a complexation at specific RNA sites, which may involve removal of water ligands from the ion's first hydration shell; an intermediate case of so-called "surface ions" has also been discussed.[29] Ion coordination, especially of Mg^{2+}, at specific sites is often involved in catalytic function,[4,5] but for (catalytically inactive) tRNA chelation of cations has been questioned.[1] Highly specific and effective cleavage of the D-loop by Pb^{2+} ions has been reported for yeast $tRNA^{Phe}$ both in solution and in crystals, and ions occupying the binding pocket in the D-TΨC region have been detected by X-ray crystallography.[30] Some other tRNAs containing the same canonical structural motif were also found to be cleaved in the D-loop by different divalent ions at elevated concentrations.[31,32] So, it has been assumed by conjecture that the same binding pocket also specifically accommodates Mg^{2+} ions. However, for many tRNAs including $tRNA^{Lys}$ investigated here, ion-induced cleavage was observed to be rather unspecific if the classical features of tertiary structure mentioned above are not present.[33] Thus, binding of Mg^{2+} ions to these tRNAs under physiologically relevant conditions can be assumed to be rather nonspecific, and the affinity is primarily governed by electrostatic interactions.[10,34,35] In addition to cation charge, the stability of compact folded RNAs with high local charge density may be sensitive to ion size even if the ions are not directly complexed.[16] Moreover, because of their preference for certain ligands, transition metal ions tend to bind more strongly to particular nucleotides, especially guanine.[36−39]

To examine the effects of ion valence, size, and electronic shell structure on the folding of tRNA, we have chosen a set of ions of different types, namely, K^+, Na^+, Mg^{2+}, Ca^{2+}, Mn^{2+}, Zn^{2+}, Tb^{3+}, and Eu^{3+}. We have taken the unmodified transcript of human mt $tRNA^{Lys}$ as a model RNA because of its delicate equilibrium between two folded conformations that makes it a sensitive probe of free energy perturbations. The first four types of ions are the physiologically most abundant monovalent and divalent ions; the latter four are frequently used in investigations of RNA folding pathways. Mn^{2+} and Zn^{2+} are transition metal ions that also play important roles in biology.[40−42] Mn^{2+}, with its charge/volume ratio similar to Mg^{2+}, is often employed in lieu of Mg^{2+} in various biochemical investigations. Likewise, the lanthanide ions Tb^{3+} and Eu^{3+} have been used as counterions to replace Mg^{2+} and also as probes of high-affinity metal binding sites in footprinting experiments.[43] Moreover, their luminescent properties can be exploited for monitoring conformational changes.[44−46] Altogether, the array of metal ions investigated here have allowed us to study the effects of positively charged ions on RNA folding by varying the coordination properties as well as the charge-to-volume ratio. Indeed, both of these properties were found to significantly affect tRNA stabilization.

EXPERIMENTAL PROCEDURES

tRNA Sample Preparation and Chemicals. Dye-labeled construct of the unmodified transcript of human mt $tRNA^{Lys}$ was prepared as described previously, except that Alexa647 was taken as FRET acceptor instead of Cy5.[15,27] Briefly, RNA fragments were purchased from IBA (Göttingen, Germany); Cy3 and Alexa647 were introduced into separate oligos by postsynthetic NHS coupling to aminolinker-carrying deoxythymidine nucleotides corresponding to positions 4 and 41, respectively, in the full length tRNA.[27] Finally, the tRNA construct was assembled from the RNA fragments by splint ligation.[47,48]

All chloride metal salts of the highest available purity were purchased from Sigma-Aldrich (Germany) as powder and dissolved in distilled water (Fluka, Taufkirchen, Germany). Except for lanthanide ions, 50 mM Tris-HCl buffer, pH 7.4, was used for tRNA sample dilution down to concentrations of ∼100 pM. 100 mM stock solutions of lanthanide ions, $TbCl_3$ and $EuCl_3$, were prepared in MES-HCl buffer (50 mM, pH 3.0) to avoid aggregation. MES buffer at pH 6.5 was used for fluorescence measurements with highly diluted lanthanide ions. The tRNA solutions were heated to 60 °C for 3 min and then slowly cooled to room temperature prior to the measurements. Metal salt

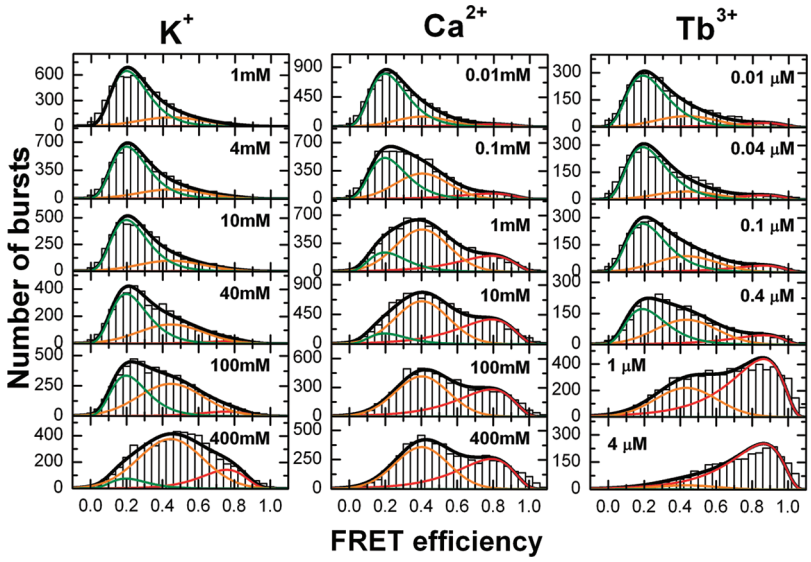

Figure 2. FRET efficiency histograms of freely diffusing Kwt $tRNA^{Lys}$ molecules at six different concentrations of K^+, Ca^{2+}, and Tb^{3+} ions. Green, yellow, and red lines represent the best-fit model distributions of the **U**, **E**, and **C** states, respectively; the solid lines show the sums of all three distributions. The approximate average FRET efficiency values are 0.25, 0.43, and 0.7 for the **U**, **E**, and **C** states, respectively: the exact values for each type of ion are given in the Supporting Information.

solutions were added afterward in the appropriate amounts to achieve the desired ion concentrations.

Single-Molecule FRET Measurements. Single-molecule fluorescence measurements were performed on freely diffusing tRNA using a home-built confocal microscope based on an Zeiss Axiovert 135 TV frame with two-channel detection.[14,15,49] Probe solutions were placed in sandwich cells consisting of two glass cover slides spaced apart by ~150 μm thick double-sided adhesive tape. Alternating excitation of Cy3 (donor) and Alexa647 (acceptor) dyes with 532 nm (green) and 633 nm (red) laser lines, correspondingly, was achieved with an acousto-optical tunable filter (AOTF, AA Opto-Electronic, Orsay, France). The repetition rate was set to 10 kHz with a duty cycle of 70:30 for green and red excitation, respectively; data acquisition was blocked for 5 μs during color switching to avoid temporal cross-talk. The fluorescence emission was collected by a water-immersion objective (Zeiss C-Apochromat 63×/1.2w, Zeiss, Oberkochen, Germany), passed through a pinhole 100 μm in diameter and separated into donor (550−610 nm) and acceptor (650−750 nm) channels. Photons were detected with avalanche photodiodes (SPCM-CD 3017, PerkinElmer, Boston, MA) and counted within the appropriate excitation periods using a multifunctional data acquisition card (NI PCI-6229, National Instruments, München, Germany).

Data analysis was performed with in-house developed software using Matlab (MathWorks, Natick, MA) and C++ (Borland, Cupertino, CA). Donor and acceptor photons were assigned based on the arrival time within each 100 μs excitation cycle and binned into photon numbers corresponding to the donor and acceptor intensities under green excitation, I_D^{Gr} and I_A^{Gr}, and red excitation, I_D^{Rd} and I_A^{Rd}. All intensities were corrected for background, spectral cross-talk, and detection efficiency. Bursts with durations between 0.2 and 2 ms and more than 50 photon counts were selected for FRET analysis. FRET efficiency values, E, were calculated according to the expression $E = I_A^{Gr}/(I_D^{Gr} + I_A^{Gr})$. Rejection of improper-labeled or bleached RNA molecules was accomplished based on the stoichiometry parameter $S = (I_D^{Gr} + I_A^{Gr})/(I_D^{Gr} + I_A^{Gr} + I_A^{Rd})$.[50]

RESULTS

Thermodynamic Model of Ion-Induced Stabilization of $tRNA^{Lys}$. We investigated conformational changes of the unmodified transcript of human mt $tRNA^{Lys}$, denoted as Kwt, upon titration with different cations. By using a fluorescence microscope with single-molecule sensitivity,[49] we measured the donor and acceptor intensities of dye-labeled Kwt molecules upon donor excitation while they diffused through the confocal spot within typically less than 1 ms. From these several thousand short bursts of intensity, we calculated FRET efficiencies of each Kwt molecule separately and compiled them in FRET efficiency histograms, in which the number of molecules found within a range of FRET values is plotted against the FRET value itself (Figure 2). Such histograms were determined with excellent statistical accuracy for up to 10 different cation concentrations and fitted by superpositions of the **U**, **E**, and **C** state distributions at low, intermediate, and high FRET efficiency values, respectively. Although the three subpopulations are largely overlapping, their existence is evident from comparing the FRET efficiency histograms at different ion concentrations. The structural properties of the three states have been thoroughly discussed in previous papers.[15,27] Typical examples of FRET efficiency histograms of the unmodified $tRNA^{Lys}$ construct Kwt are presented in Figure 2 for selected concentrations of K^+, Ca^{2+}, and Tb^{3+} ions; FRET efficiency histograms for the other ions are given in the Supporting Information. To compute the fractional populations of the three different conformations from the FRET histograms, we modeled their FRET distributions as in our previous work,[14,15] namely, by log−normal functions for the low-FRET **U** and high-FRET **C** states and a normal Gaussian function for the **E** state at the intermediate FRET efficiencies. Because of broad and overlapping subpopulations, the following constraints on the distribution parameters have been used in a global fit in order to decrease the fit errors: On the basis of the experimental observations that the average FRET efficiencies and widths of the distributions of **U**, **E**, and **C** did not change noticeably with ion

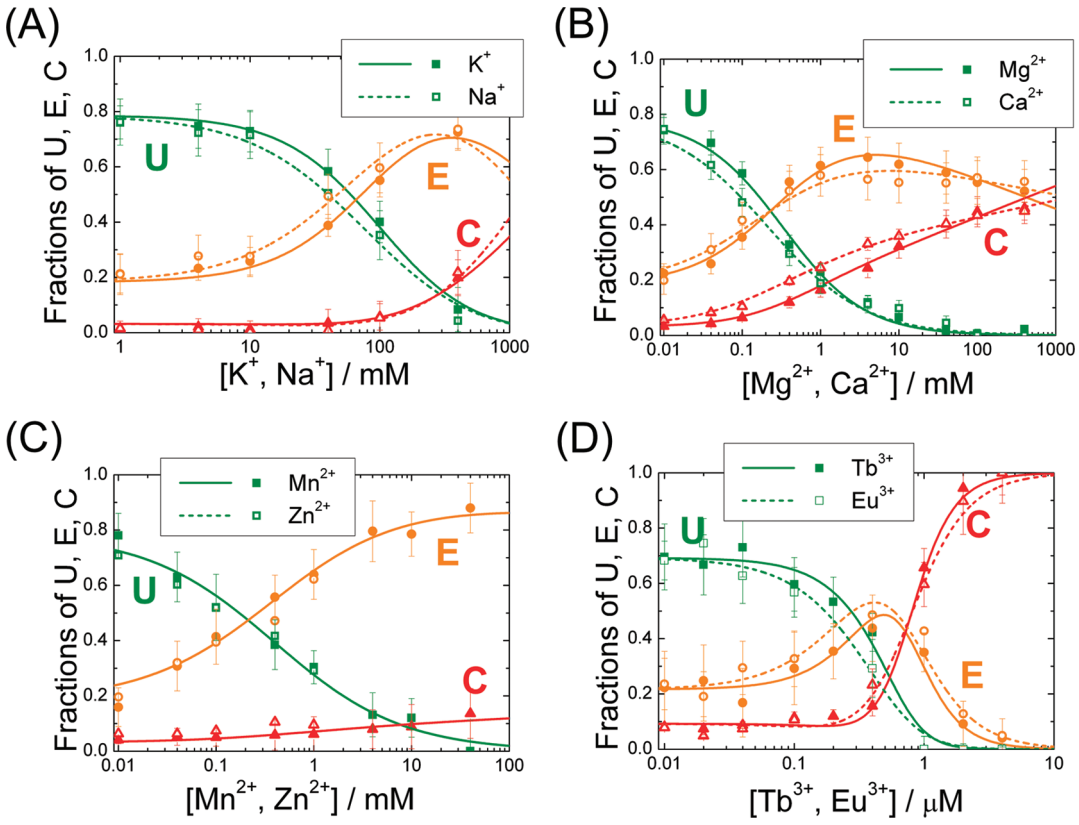

Figure 3. Kwt $tRNA^{Lys}$ fractional populations of the **U**, **E**, and **C** states as a function of alkali (A), alkaline earth (B), transition (C), and lanthanide (D) metal ions. Lines represent results from fitting the data with the thermodynamic model discussed in the text.

concentration, they were kept constant in global fits at all concentrations of a particular cation, so that only the areas and, consequently, the relative populations were allowed to vary. Excellent agreement was obtained between the model fits (lines in Figure 2 and Figures S2−S8 in the Supporting Information) and the experimental data for all concentrations of different ions. The global fit parameters of the averaged FRET efficiencies and full widths at half-maxima (fwhm) of the respective model functions are given in the Supporting Information. These generally agree with our previous work;[15,27] however, some variations of the peak position of the rather flexible **E** state can be noticed for different types of cations. The widths of the **E** and **C** subpopulations are quite broad due to dye photophysics, sample static heterogeneity, or conformational changes on the time scale of molecule diffusion in addition to photon shot noise. The physical origins of this broadening require careful further investigations, which is not the focus of the present work, however. Most prominent changes in response to different cations were observed for the areas of the distributions, from which we calculated the fractional populations of the **U**, **E**, and **C** states. In Figure 3, the fractional populations of the **U**, **E**, and **C** states of Kwt are plotted as a function of ion concentrations for different types of cations.

In the quantitative analysis of the free energy changes, we employed a thermodynamic framework presented earlier.[15] It includes altogether six states because it is assumed that the three conformations, **U**, **E**, and **C**, can be described as a sum of "ion-free" ($\mathbf{U}_0$, $\mathbf{E}_0$, and $\mathbf{C}_0$) and "ion-bound" (denoted as $\mathbf{U}_{ion}$, $\mathbf{E}_{ion}$, and $\mathbf{C}_{ion}$) states (Figure 1B). Notably, the terms "ion-free" or "ion-bound" refer only to the absence or presence of those ions with which the RNA was titrated but not to the buffer ions (here $Tris^+$) that were kept at a constant concentration. Intuitively, we expect that the ion-free states are populated at low ion concentration, whereas the ion-bound states dominate at higher ion concentrations. However, it is important to note that, in our smFRET experiments, we cannot independently distinguish between the structurally similar ion-free and ion-bound states; so, only their sum is measured for each conformation in the form of fractional populations. The free energy difference between the ion-free states accounts for the intrinsic stability change due to structural compaction in the absence of ion stabilization. The equilibria between the states **U**, **E**, and **C** are governed by the free energy differences between the ion-free conformations, ΔG^0_{ij}, and the free energy changes of ion-induced folding of each state, $\Delta G_i(\text{ion})$. Here, i and j are labels referring to the **U**, **E**, or **C** states, respectively. The populations, $[i]$, are governed by Boltzmann statistics

$$\frac{[i_0]}{[j_0]} = \exp\left(-\frac{\Delta G^0_{ij}}{RT}\right) \quad (1)$$

$$\frac{[i_0]}{[i_{ion}]} = \exp\left(-\frac{\Delta G_i(\text{ion})}{RT}\right) \quad (2)$$

where R and T represent the gas constant and the absolute temperature, respectively. To model the free energy changes of the RNA conformational states upon ion binding, we employed the widely used Hill equation

$$\Delta G_i(\text{ion}) = \Delta G^0_i + n_i RT \ln[\text{ion}] \quad (3)$$

dx.doi.org/10.1021/bi101804t |*Biochemistry* 2011, 50, 3107–3115

Table 1. Parameters n_i and ΔG_i^0 (in kcal/mol at 1 M Concentration of the Titrated Ion) Were Obtained from the Analysis of smFRET Fractional Populations Using the Thermodynamic Model Described in the Text

	n_E	n_C	ΔG_E^0 (kcal/mol)	ΔG_C^0 (kcal/mol)
K^+	1.4 ± 0.1	2.0 ± 0.1	3.0 ± 0.2	5.5 ± 0.3
Na^+	1.2 ± 0.1	2.0 ± 0.1	3.0 ± 0.1	6.4 ± 0.5
Mg^{2+}	0.79 ± 0.01	0.99 ± 0.01	5.1 ± 0.1	7.3 ± 0.2
Ca^{2+}	0.68 ± 0.02	0.78 ± 0.02	4.7 ± 0.1	6.6 ± 0.3
Mn^{2+}	0.65 ± 0.02	0.75 ± 0.02	4.6 ± 0.4	5.0 ± 0.3
Tb^{3+}	1.7 ± 0.1	4.0 ± 0.2	8.8 ± 2.0	19.8 ± 3.3
Eu^{3+}	1.3 ± 0.1	3.1 ± 0.1	7.5 ± 1.4	16.3 ± 2.1

Recently, Leipply and Draper have thoroughly discussed the applicability and interpretation of the Hill equation and coefficient.[17] Typically, the Hill equation is applied to model conformational transitions, $[i_0 + i_{ion}] \leftrightarrow [j_0 + j_{ion}]$, represented by the horizontal arrows in Figure 1A. Here, we use eq 3 as an empirical relationship to describe the change of the ion-bound states only, $\mathbf{U}_{ion}$, $\mathbf{E}_{ion}$, and $\mathbf{C}_{ion}$, as a function of ion concentration. Specifically, the n_i parameter is not interpreted as a stoichiometric coefficient representing the number of ions binding to the RNA; the meaning of this parameter will be explained in the Discussion section. While only the fractional populations are calculated, reference energy levels for the ion-free and ion-bound states have to be defined by hand. Thus, ΔG_U^0 and ΔG_U(ion) were set equal to zero, and the free energy changes of the $\mathbf{E}_{ion}$ and $\mathbf{C}_{ion}$ states were calculated relative to the unfolded state:

$$\Delta G_E = \Delta G_{UE}^0 + \Delta G_E^0 + n_E RT \ln[\text{ion}],$$
$$\Delta G_C = \Delta G_{UC}^0 + \Delta G_C^0 + n_C RT \ln[\text{ion}] \quad (4)$$

By using eqs 1−4, a set of equations for the fractional populations $K_i = [i_0 + i_{ion}]/\Sigma[i_0 + i_{ion}]$ of the **U**, **E**, and **C** states (see Supporting Information for mathematical details) was expressed as a function of ion concentration with only six parameters, namely, n_E, n_C, ΔG_E^0, ΔG_C^0, ΔG_{UE}^0, and ΔG_{UC}^0, varied in the fit for each set of ion concentration dependent data. Moreover, the last two parameters, i.e., the free energy differences between the ion-free states, are independent of the type of ion (but dependent on the other buffer conditions, such as pH, for example). So, these two parameters were determined in a global fit of all titration sets obtained at the same pH. The remaining four parameters were individually fitted for each type of ion. The fit results are shown in Figure 3 as lines, and the values of n_E, n_C, ΔG_E^0, and ΔG_C^0 are given in Table 1. The fit curves nicely follow the experimental data for different types of ions in the full range of concentrations, which gives confidence to the applicability of our thermodynamic model.

Interaction of RNA with Na^+ and K^+. Alkali ions Na^+ and K^+ are of key importance for biological organisms. Many RNA structures fold into their native conformations even if only these ions are present.[16,51] However, concentrations of several hundred millimolar are typically required for the functional folding of tRNAs in the absence of divalent cations, which by far exceeds physiological concentrations.[10] In Figure 3A, the fractions of the **U**, **E**, and **C** states of Kwt $tRNA^{Lys}$ are plotted as a function of Na^+ and K^+ ion concentrations. The unfolded state dominates at low cation concentration. Only above 10 mM, the **E** state increases at the expense of the **U** state; the functional **C** state appears only above 100 mM but still does not exceed the **E** state in the studied range of monovalent cation concentrations. From the nonlinear least-squares fit of the thermodynamic model to the data, shown as lines in the Figure 3A, we determined free energy differences between the ion-free states $\mathbf{U}_0$, $\mathbf{E}_0$, and $\mathbf{C}_0$, ΔG_{UE}^0, and ΔG_{UC}^0, as 0.46 ± 0.01 and 1.50 ± 0.06 kcal/mol, respectively. To evaluate the effect of monovalent buffer ions to the free energy changes, we have also titrated the $Tris^+$ concentration from 10 to 250 mM; the FRET histograms and fractional populations as a function of $Tris^+$ concentration are shown in Figure S10 of the Supporting Information. There, significant stabilization of the **E** state by $Tris^+$ ions alone starts at higher concentrations (>100 mM) than by K^+ or Na^+ (>10 mM) in the presence of 50 mM $Tris^+$.

Interaction of RNA with Mg^{2+} and Ca^{2+}. Divalent ions are known to stabilize RNA tertiary folds more efficiently than monovalent ones. Indeed, the **E** state becomes the dominant species already at concentrations above ~0.2 mM and the **C** state above ~500 mM for either Mg^{2+} or Ca^{2+} (Figure 3B). The analysis of the titration behavior revealed some minor preferences for Ca^{2+} ions at intermediate ion concentrations, while the preference inverts toward Mg^{2+} ions at higher ion concentrations (Figure 3B). This observation is difficult to explain just by the difference in ionic radii of divalent ions (1.00 Å for Ca^{2+} versus 0.72 Å for Mg^{2+}). The total number of ions necessary to compensate the negative charges of the RNA backbone is by a factor of 2 smaller for divalent than for monovalent ions. Consequently, the entropic penalty due to binding to the RNA is reduced by a factor of 2. Therefore, because of the alleviated space constraints, the effect of ion size might be less pronounced for divalent ions. However, weak specific binding sites or kinetic traps may, in principle, exist for divalent ions, especially in the deep grooves of the RNA and at helical junctions. In those cases, the interaction may occur via hydrogen bonding between the RNA and first hydration layer around the ions. While Mg^{2+} coordinates up to six water molecules, the coordination number of Ca^{2+} ranges from 6 to 9, which could explain the small preference for their binding to the **C** state at intermediate ion concentrations and slightly narrower FRET distributions (see Table S1 in Supporting Information).

Interaction of RNA with Transition Metal Cations. For smFRET studies of the effect of transition metal cations on RNA stability, we chose Mn^{2+} and Zn^{2+}, for which abundant data exist to which our results can be compared.[34,35,52,53] Because these ions cause significant dynamic fluorescence quenching, FRET efficiency measurements were only possible up to 1 mM for Zn^{2+} ions and up to 40 mM for Mn^{2+} ions. The fractional populations of the corresponding **U**, **E**, and **C** states as a function of ion concentration perfectly coincide for both counterions (Figure 3C). We note that quenching influences both fluorophores, donor and acceptor, equally, so the quenching effect cancels in the calculation of FRET efficiency values, and the FRET efficiency histograms are not affected (Figure S6 in Supporting Information). Compared to the divalent earth alkaline ions Mg^{2+} and Ca^{2+}, a clear difference of the folding properties of the **U**, **E**, and **C** states is apparent for the transition metals: the **E** state significantly increases at the expense of the **U** state and levels off at high concentrations (Figure 3C), whereas the **C** state does not exceed a fraction of 10% even at the highest ion concentrations used (40 mM). This behavior indicates that Mn^{2+} ions may interact specifically with the non-native **E** conformation, which is somewhat unexpected because Mn^{2+} ions are often considered as good substitutes for Mg^{2+} ions and

widely used as paramagnetic probes in EPR- and NMR-based spectroscopic studies of RNA binding.[54,55] With the same coordination number of 6 and a similar ionic radius (~0.81 Å) as Mg^{2+}, Mn^{2+} has a higher preference for coordination with nitrogen instead of oxygen ligands than magnesium. Zn^{2+} ions, too, preferentially bind to nitrogenous ligands, with coordination numbers ranging from 4 to 6.[56] Up to 4 of 6 water molecules in the inner sphere of Mn^{2+} are easily replaced by other ligands.[56] Quantum-chemical calculations on different pentahydrated divalent ions, in particular Mg^{2+} and Mn^{2+}, bound to the *N7* atom of guanine,[39] revealed that the replacement of water molecules by guanine was more favorable for Mn^{2+} than for Mg^{2+}. This effect was attributed to an enhanced electron density in the 3d orbitals due to back-donation from the guanine aromatic ring.

Interaction of RNA with Trivalent Cations. Lanthanide ions are used in RNA chemistry as versatile probes of RNA secondary and tertiary structure and to identify high-affinity metal ion binding sites. We have compared Tb^{3+} and Eu^{3+} ions to the monovalent and divalent ions for their ability to fold human mt $tRNA^{Lys}$. Because Tb^{3+} accelerates hydrolysis of the RNA backbone at neutral pH,[57] single-molecule FRET experiments were carried out in MES buffer at pH 6.5. Under these conditions, we found that the thermodynamic equilibrium was shifted slightly toward the folded conformations; the parameters ΔG^0_{UE} and ΔG^0_{UC} are different from measurements in standard RNA buffer. Otherwise, a similar folding behavior was observed as for titrating the tRNA molecule with Ca^{2+} ions (data not shown). The binding of Tb^{3+} and Eu^{3+} ions was studied in the range from 0.01 up to 4 μM; selected FRET efficiency histograms are shown in Figure 2C. From the resulting fractional populations of **U**, **E**, and **C** in Figure 3D it is evident that the trivalent ions are even more effective than the divalent ones in stabilizing compact RNA folds: the transition from **U** to **E** to **C** states occurs in the sub-micromolar range, as was also observed for other RNAs titrated with trivalent cations.[58] Notably, the transition, which starts at ~0.1 μM, is much sharper than for the other studied ions, and above 5 μM, the Kwt $tRNA^{Lys}$ is completely folded into the **C** state. The fit of fractional state populations with the thermodynamic model revealed values of ΔG^0_{UE} and ΔG^0_{UC} equal to 0.28 ± 0.01 and 0.79 ± 0.01 kcal/mol, respectively. The observed small deviations in the Tb^{3+} or Eu^{3+} titration behavior are within the experimental error.

DISCUSSION

RNA molecules possess very rugged free energy landscapes because they often form alternative stable secondary structure elements, giving rise to multiple metastable conformations of similar free energy. The tRNA molecule studied here possesses two thermodynamically stable folded conformations, the ratio of which can be altered by post-transcriptional modifications or mutations.[26,59] Notably, one of these conformations is not an on-pathway intermediate en route to the other one, so folding from the **U** state may generate either the **E** or the **C** state. Which conformational state is better stabilized by ions is, thus, determined by the interplay between structural rearrangements and ion binding. The thermodynamic model presented in this paper describes the equilibrium between all three states and dissects the complicated response of RNA with counterions into the interaction of ions with each particular conformation, which is again separated into an ion-free and an ion-bound state. Both states are assumed to be structurally similar; however, a certain compaction of a given state with increasing ion concentration is entirely possible.[60−64] Indeed, we have observed such an effect in smFRET measurements on the intermediate state of a Diels−Alderase ribozyme.[14] For Kwt $tRNA^{Lys}$, a shift of the mean FRET efficiencies of the **E** and **C** states is not apparent in our FRET histograms, probably because the effect is relatively small compared to the widths of the distributions. A hint of a compaction of conformations may only be observed at the highest ion concentrations. In any case, the free energy difference, ΔG^0_{UE} and ΔG^0_{UC}, of compaction from the $\mathbf{U}_0$ to $\mathbf{E}_0$ and to $\mathbf{C}_0$ states in the presence of buffer ions is smaller than the energy of the cation-mediated RNA stabilization. Consequently, the free energy changes due to compaction within the **E** or **C** states will be even smaller.

The excellent fits of our model to all experimental data provide confidence on the thermodynamic model, but a proper interpretation of the extracted parameters is required. An important quantity in this context is the relative change of the free energy difference between two conformational states *i* and *j*, $\Delta\Delta G_{ij}$, caused by changing counterion concentrations, which is calculated as

$$\Delta\Delta G_{ij} \approx -RT \ln(K_j/K_i) \quad (5)$$

where K_i is the fractional population of state *i*. In Figure 4 (upper panel), we have plotted the free energy changes, $\Delta\Delta G$, for the two folded conformations **E** and **C** for different type of ions as a function of their concentration. A monotonic decrease of $\Delta\Delta G$ is observed with increasing ion concentration. The intersection with the zero line corresponding to the concentration at state **E** or **C** is equally populated as **U**, while the crossing of $\Delta\Delta G_{UC}$ and $\Delta\Delta G_{UE}$ marks the concentration above which the **C** state becomes the dominant population. Next, we discuss the meaning of the parameter n_i in the thermodynamic model. Spectroscopic measurements do not resolve the transition from ion-free to ion-bound state directly, so the interpretation of the n_i parameter as a Hill coefficient or cooperativity parameter is not appropriate. Rather, the free energy changes in the thermodynamic cycle depicted in Figure 1B ought to be interpreted in terms of preferential interaction coefficients, Γ, which represent an excess number of cations in close proximity to the RNA molecule over the bulk value.[65] However, only the difference, $\Delta\Gamma_{ij}$, between Γ_i of different conformations is observed in experiments in which the relative change in the populations of RNA conformations (in our case we have referred all changes to the unfolded state) is measured. According to Grilley et al.,[60] $\Delta\Gamma$ can be expressed as

$$\Delta\Gamma \approx -\frac{1}{RT}\frac{\partial \ln K_{obs}}{\partial \ln[ion]} = \frac{\partial \Delta G_{obs}}{\partial \ln[ion]} \quad (6)$$

So, taking advantage of single-molecule measurements to resolve individual subpopulations, we can calculate conformationally pure $\Delta\Gamma_{ij}$ coefficients based on the semiempirically determined fractional populations. The resulting dependencies of $\Delta\Gamma_{UE}$ and $\Delta\Gamma_{UC}$ on the ion concentrations are presented in Figure 4 (lower panel) for monovalent, divalent, and trivalent ions. It is obvious from the observed saturation of the $\Delta\Gamma_{ij}$ parameter that the n_j parameters correspond to the maximum values of $\Delta\Gamma_{ij}$ in the limit of high ion concentration. However, as noted in ref 60, the analysis in terms of preferential interaction coefficients is applicable only in the presence of excess monovalent ions over multivalent ones. So, at very high concentrations of titrated ions (>10 mM), the real $\Delta\Gamma_{ij}$ might deviate from the curves shown in Figure 4. Indeed, as soon as the number of excess ions in close proximity to the RNA molecule reaches saturation, a further increase in bulk ion concentration

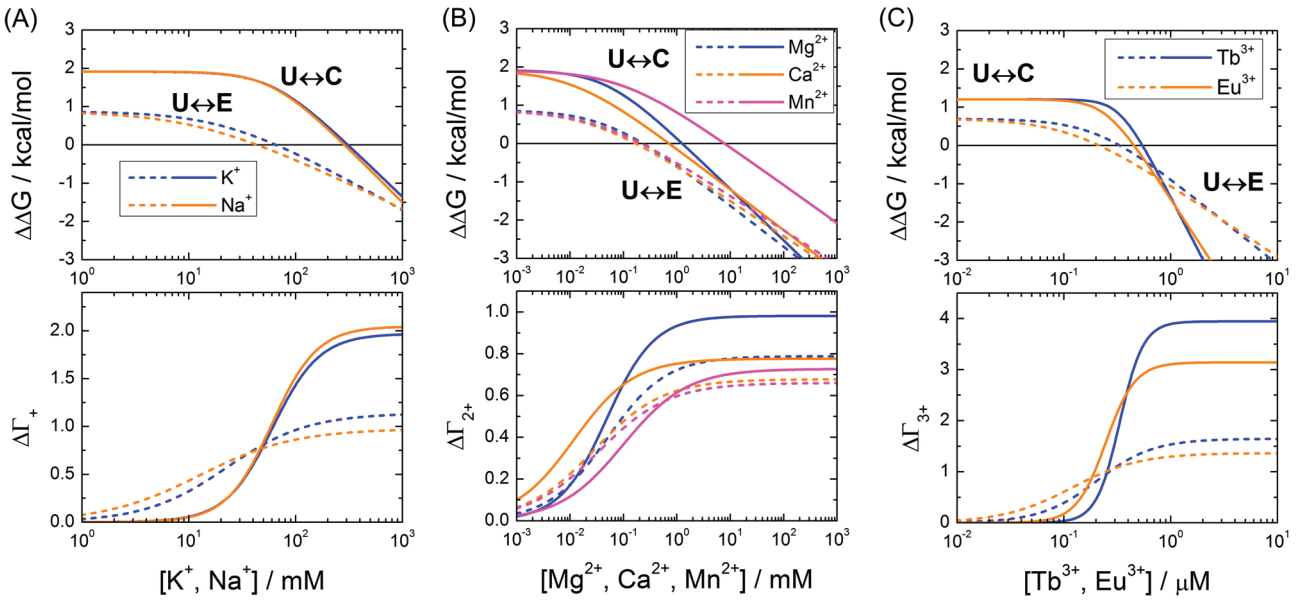

Figure 4. Difference in folding free energy, $\Delta\Delta G$ (upper panel), and difference in preferential interaction coefficient, $\Delta\Gamma$ (lower panel), for the U ↔ E (dashed lines) and U ↔ C (solid lines) transitions as a function of monovalent (A), divalent (B), and trivalent (C) ion concentration.

should lead to a decrease of the values of $\Delta\Gamma_{ij}$. Unfortunately, at those concentrations, the unfolded state is practically not populated, and therefore, an accurate extraction of $\Delta\Delta G_{UE}$ and $\Delta\Delta G_{UC}$ is not feasible. At low concentrations, the values of $\Delta\Gamma_{ij}$ approach zero, as expected.[17]

A comprehensive analysis of RNA−ion energetics is exceedingly difficult; yet, the difference between monovalent and multivalent ion stabilization is rather well explained by simple counterion condensation theory.[66,67] For tRNAs, the sophisticated tertiary structure gives rise to regions with locally high charge density, where coordination of ions with the RNA backbone and bases is possible via water molecules. Assuming rather unspecific interaction of ions with the unfolded state of RNA, specific ion binding to only one of the two folded conformations **E** and **C** of $tRNA^{Lys}$ should result in their dissimilar behavior upon titration with ions of the same charge. A common observation for all types of ions in Figure 4 is that the net ion uptake is larger and steeper for conformation **C**, which has the highest charge density. While we do not observe much variation among different monovalent and trivalent ions, divalent ions show a more interesting behavior, especially upon binding to the **C** state. Thus, the largest and steepest net ion uptake is observed for Mg^{2+} ions, likely because of their small size. According to entropic considerations, ions with a smaller radius may approach the RNA surface more closely and, thereby, screen the negative charge more effectively.[16] Moreover, Mg^{2+} uptake starts practically at the same concentration for both the **E** and **C** conformation. With the exception of Ca^{2+} ions, this behavior was not observed for any other type of ions studied, for which the **E** state appears to be surrounded by ions starting at lower concentrations than for the **C** state. In the presence of Ca^{2+} ions, both folded conformations started to become stabilized at lower concentrations than for Mg^{2+}, although the **C** state takes up Ca^{2+} ions at lower concentrations than the **E** state. The larger coordination number of Ca^{2+} ions may be responsible for this effect. However, stabilization is not as efficient as for Mg^{2+} ions at higher concentrations. The smallest difference of the ion-mediated stabilization of RNA conformations was observed for Mn^{2+} ions. There, the final net ion uptake and steepness were practically identical for both **E** and **C** conformations. Presumably, Mn^{2+} ions bind to nitrogen atoms on the bases and, apart from electrostatic screening, do not participate in tertiary interactions.

In conclusion, we have applied a thermodynamic model to smFRET data to quantitatively analyze the conformation-dependent stabilization of the unmodified transcript of human mt $tRNA^{Lys}$ by counterions. In agreement with previous ensemble measurements,[6,13,16,68] we have observed that the ion's valence state is the primary parameter for tRNA stabilization. Also, secondary effects such as ion size and coordination properties to specific ligand were noticed for ions of the same charge, especially for divalent ions. However, in contrast to the two-state RNA transitions typically studied on the ensemble level, we have studied a system that can assume three well-distinguishable conformations, namely the unfolded and two differently folded states. This property allowed us to directly compare the free energy changes of the cation-governed tertiary stabilization between the two folded states of different compactness. The analysis presented here may be generally applicable to studies of counterion effects on RNA folding equilibria.

■ ASSOCIATED CONTENT

Supporting Information. Figures showing single-molecule FRET efficiency histograms of freely diffusing Kwt $tRNA^{Lys}$ molecules taken in buffers containing different concentrations of all ions studied in recent work, a table providing parameters of the fitting function of smFRET efficiency histograms, and mathematical details of the thermodynamic model. This material is available free of charge via the Internet at http://pubs.acs.org.

■ AUTHOR INFORMATION

Corresponding Author

*Tel: +49 (0)721 608-45341. Fax: +49 (0)721 608-48480. E-mail: a.kob@kit.edu.

Present Addresses

[#]Institute of Experimental Physics, University of Ulm, 89069 Ulm, Germany.

[&]Department of Chemistry and Biochemistry, University of California, Santa Cruz, Santa Cruz, CA 95064.

Funding Sources

This work was supported by the Volkswagen Foundation (VW-I/82549), the Deutsche Forschungsgemeinschaft (DFG) (HE 3397/3 and CFN), and the Fonds der Chemischen Industrie. Martin Hengesbach acknowledges funding by the Landesgraduiertenförderung Baden-Württemberg.

REFERENCES

(1) Draper, D. E., Grilley, D., and Soto, A. M. (2005) Ions and RNA folding. *Annu. Rev. Biophys. Biomol. Struct. 34*, 221–243.

(2) Woodson, S. A. (2005) Metal ions and RNA folding: a highly charged topic with a dynamic future. *Curr. Opin. Chem. Biol. 9*, 104–109.

(3) Brion, P., and Westhof, E. (1997) Hierarchy and dynamics of RNA folding. *Annu. Rev. Biophys. Biomol. Struct. 26*, 113–137.

(4) Fedor, M. J. (2002) The role of metal ions in RNA catalysis. *Curr. Opin. Struct. Biol. 12*, 289–295.

(5) Pyle, A. M. (2002) Metal ions in the structure and function of RNA. *J. Biol. Inorg. Chem. 7*, 679–690.

(6) Cole, P. E., Yang, S. K., and Crothers, D. M. (1972) Conformational changes of transfer ribonucleic acid. Equilibrium phase diagrams. *Biochemistry 11*, 4358–4368.

(7) Römer, R., and Hach, R. (1975) tRNA conformation and magnesium binding. A study of a yeast phenilalanine-specific tRNA by a fluorescent indicator and differential melting curves. *Eur. J. Biochem. 55*, 271–284.

(8) Stein, A., and Crothers, D. M. (1976) Conformational changes of transfer RNA. The role of magnesium(II). *Biochemistry 15*, 160–168.

(9) Fang, X., Pan, T., and Sosnick, T. R. (1999) A thermodynamic framework and cooperativity in the tertiary folding of a Mg2+-dependent ribozyme. *Biochemistry 38*, 16840–16846.

(10) Misra, V. K., and Draper, D. E. (2000) Mg(2+) binding to tRNA revisited: the nonlinear Poisson-Boltzmann model. *J. Mol. Biol. 299*, 813–825.

(11) Misra, V. K., and Draper, D. E. (2001) A thermodynamic framework for Mg2+ binding to RNA. *Proc. Natl. Acad. Sci. U.S.A. 98*, 12456–12461.

(12) Grilley, D., Soto, A. M., and Draper, D. E. (2006) Mg2+-RNA interaction free energies and their relationship to the folding of RNA tertiary structures. *Proc. Natl. Acad. Sci. U.S.A. 103*, 14003–14008.

(13) Koculi, E., Hyeon, C., Thirumalai, D., and Woodson, S. A. (2007) Charge density of divalent metal cations determines RNA stability. *J. Am. Chem. Soc. 129*, 2676–2682.

(14) Kobitski, A. Y., Nierth, A., Helm, M., Jäschke, A., and Nienhaus, G. U. (2007) Mg2+-dependent folding of a Diels-Alderase ribozyme probed by single-molecule FRET analysis. *Nucleic Acids Res. 35*, 2047–2059.

(15) Kobitski, A. Y., Hengesbach, M., Helm, M., and Nienhaus, G. U. (2008) Sculpting of an RNA Conformational Energy Landscape by a Methyl Group Modification - A Single-Molecule Study. *Angew. Chem., Int. Ed. 47*, 4326–4330.

(16) Lambert, D., Leipply, D., Shiman, R., and Draper, D. E. (2009) The influence of monovalent cation size on the stability of RNA tertiary structures. *J. Mol. Biol. 390*, 791–804.

(17) Leipply, D., and Draper, D. E. (2010) Dependence of RNA tertiary structural stability on Mg2+ concentration: interpretation of the Hill equation and coefficient. *Biochemistry 49*, 1843–1853.

(18) Frauenfelder, H., Sligar, S. G., and Wolynes, P. G. (1991) The energy landscapes and motions of proteins. *Science 254*, 1598–1603.

(19) Nienhaus, G. U., Müller, J. D., McMahon, B. H., and Frauenfelder, H. (1997) Exploring the Conformational Energy Landscape of Proteins. *Physica D 107*, 297–311.

(20) Russell, R., Zhuang, X., Babcock, H. P., Millett, I. S., Doniach, S., Chu, S., and Herschlag, D. (2002) Exploring the folding landscape of a structured RNA. *Proc. Natl. Acad. Sci. U.S.A. 99*, 155–160.

(21) Zarrinkar, P. P., and Williamson, J. R. (1994) Kinetic intermediates in RNA folding. *Science 265*, 918–924.

(22) Thirumalai, D., and Woodson, S. A. (1996) Kinetics of Folding of Proteins and RNA. *Acc. Chem. Res. 29*, 433–439.

(23) Treiber, D. K., Rook, M. S., Zarrinkar, P. P., and Williamson, J. R. (1998) Kinetic intermediates trapped by native interactions in RNA folding. *Science 279*, 1943–1946.

(24) Pan, J., Thirumalai, D., and Woodson, S. A. (1997) Folding of RNA involves parallel pathways. *J. Mol. Biol. 273*, 7–13.

(25) Helm, M., Giege, R., and Florentz, C. (1999) A Watson-Crick base-pair-disrupting methyl group (m1A9) is sufficient for cloverleaf folding of human mitochondrial tRNALys. *Biochemistry 38*, 13338–13346.

(26) Helm, M., and Attardi, G. (2004) Nuclear control of cloverleaf structure of human mitochondrial tRNA(Lys). *J. Mol. Biol. 337*, 545–560.

(27) Voigts-Hoffmann, F., Hengesbach, M., Kobitski, A. Y., van Aerschot, A., Herdewijn, P., Nienhaus, G. U., and Helm, M. (2007) A methyl group controls conformational equilibrium in human mitochondrial tRNA(Lys). *J. Am. Chem. Soc. 129*, 13382–13383.

(28) Helm, M., Kobitski, A., and Nienhaus, G. U. (2009) Single-molecule Förster resonance energy transfer studies of RNA structure, dynamics and function. *Biophys. Rev. 1*, 161–176.

(29) Draper, D. E. (2004) A guide to ions and RNA structure. *RNA 10*, 335–343.

(30) Brown, R. S., Dewan, J. C., and Klug, A. (1985) Crystallographic and biochemical investigation of the lead(II)-catalyzed hydrolysis of yeast phenylalanine tRNA. *Biochemistry 24*, 4785–4801.

(31) Marciniec, T., Ciesiolka, J., Wrzesinski, J., and Krzyzosiak, W. J. (1989) Identification of the magnesium, europium and lead binding sites in E. coli and lupine tRNAPhe by specific metal ion-induced cleavages. *FEBS Lett. 243*, 293–298.

(32) Matsuo, M., Yokogawa, T., Nishikawa, K., Watanabe, K., and Okada, N. (1995) Highly specific and efficient cleavage of squid tRNA-(Lys) catalyzed by magnesium ions. *J. Biol. Chem. 270*, 10097–10104.

(33) Sissler, M., Helm, M., Frugier, M., Giege, R., and Florentz, C. (2004) Aminoacylation properties of pathology-related human mitochondrial tRNA(Lys) variants. *RNA 10*, 841–853.

(34) Walters, J. A., Geerdes, H. A., and Hilbers, C. W. (1977) On the binding of Mg2+ and Mn2+ to tRNA. *Biophys. Chem. 7*, 147–151.

(35) Gueron, M., and Leroy, J. L. (1982) Significance and mechanism of divalent-ion binding to transfer RNA. *Biophys. J. 38*, 231–236.

(36) Gao, Y. G., Sriram, M., and Wang, A. H. (1993) Crystallographic studies of metal ion-DNA interactions: different binding modes of cobalt(II), copper(II) and barium(II) to N7 of guanines in Z-DNA and a drug-DNA complex. *Nucleic Acids Res. 21*, 4093–4101.

(37) Wrzesinski, J., and Jozwiakowski, S. K. (2008) Structural basis for recognition of Co2+ by RNA aptamers. *FEBS J. 275*, 1651–1662.

(38) Millonig, H., Pous, J., Gouyette, C., Subirana, J. A., and Campos, J. L. (2009) The interaction of manganese ions with DNA. *J. Inorg. Biochem. 103*, 876–880.

(39) Oliva, R., and Cavallo, L. (2009) Frequency and effect of the binding of Mg2+, Mn2+, and Co2+ ions on the guanine base in Watson-Crick and reverse Watson-Crick base pairs. *J. Phys. Chem. B 113*, 15670–15678.

(40) Schramm, V. L., and Wedler, F. C. (1986) *Manganese in Metabolism and Enzyme Function*, Academic Press, New York.

(41) Kolev, N. G., Hartland, E. I., and Huber, P. W. (2008) A manganese-dependent ribozyme in the 3′-untranslated region of Xenopus Vg1 mRNA. *Nucleic Acids Res. 36*, 5530–5539.

(42) Mulkidjanian, A. Y., and Galperin, M. Y. (2009) On the origin of life in the zinc world. 2. Validation of the hypothesis on the photosynthesizing zinc sulfide edifices as cradles of life on Earth. *Biol. Direct 4*, 27.

(43) Harris, A. A., and Walter, N. G. (2009) in *Handbook of RNA Biochemistry* (Hartmann, R. K., Bindereif, A., Schön, A., and Westhof, E., Eds.), pp 205−213, Wiley-VCH Verlag GmbH & Co. KGaA, Weinheim.

(44) Selvin, P. R. (2002) Principles and biophysical applications of lanthanide-based probes. *Annu. Rev. Biophys. Biomol. Struct. 31*, 275–302.
(45) Yuan, F., Griffin, L., Phelps, L., Buschmann, V., Weston, K., and Greenbaum, N. L. (2007) Use of a novel Forster resonance energy transfer method to identify locations of site-bound metal ions in the U2-U6 snRNA complex. *Nucleic Acids Res. 35*, 2833–2845.
(46) Costa, D., Luísa Ramos, M., Burrows, H. D., José Tapia, M., and da Graça Miguel, M. (2008) Using lanthanides as probes for polyelectrolyte-metal ion interactions. Hydration changes on binding of trivalent cations to nucleotides and nucleic acids. *Chem. Phys. 352*, 241–248.
(47) Kurschat, W. C., Müller, J., Wombacher, R., and Helm, M. (2005) Optimizing splinted ligation of highly structured small RNAs. *RNA 11*, 1909–1914.
(48) Hengesbach, M., Kobitski, A., Voigts-Hoffmann, F., Frauer, C., Nienhaus, G. U., and Helm, M. (2008) RNA intramolecular dynamics by single-molecule FRET. *Curr. Protoc. Nucleic Acid Chem.* Chapter 11, Unit 11 12.
(49) Kuzmenkina, E. V., Heyes, C. D., and Nienhaus, G. U. (2005) Single-molecule Forster resonance energy transfer study of protein dynamics under denaturing conditions. *Proc. Natl. Acad. Sci. U.S.A. 102*, 15471–15476.
(50) Kapanidis, A. N., Lee, N. K., Laurence, T. A., Doose, S., Margeat, E., and Weiss, S. (2004) Fluorescence-aided molecule sorting: analysis of structure and interactions by alternating-laser excitation of single molecules. *Proc. Natl. Acad. Sci. U.S.A. 101*, 8936–8941.
(51) Kim, H. D., Nienhaus, G. U., Ha, T., Orr, J. W., Williamson, J. R., and Chu, S. (2002) Mg2+-dependent conformational change of RNA studied by fluorescence correlation and FRET on immobilized single molecules. *Proc. Natl. Acad. Sci. U.S.A. 99*, 4284–4289.
(52) Lindqvist, M., Sandstrom, K., Liepins, V., Stromberg, R., and Graslund, A. (2001) Specific metal-ion binding sites in a model of the P4-P6 triple-helical domain of a group I intron. *RNA 7*, 1115–1125.
(53) Shan, S. O., and Herschlag, D. (2002) Dissection of a metal-ion-mediated conformational change in Tetrahymena ribozyme catalysis. *RNA 8*, 861–872.
(54) Danchin, A., and Gueron, M. (1970) Proton magnetic relaxation study of the manganese-transfer-RNA complex. *J. Chem. Phys. 53*, 3599–3609.
(55) Hyafil, F., and Blanquet, S. (1977) Methionyl-tRNA synthetase from Escherichia coli: substituting magnesium by manganese in the L-methionine activating reaction. *Eur. J. Biochem. 74*, 481–493.
(56) Bock, C. W., Katz, A. K., Markham, G. D., and Glusker, J. P. (1999) Manganese as a replacement for magnesium and zinc: a functional comparison of the divalent Ions. *J. Am. Chem. Soc. 121*, 7360–7372.
(57) Ciesiolka, J., Marciniec, T., and Krzyzosiak, W. (1989) Probing the environment of lanthanide binding sites in yeast tRNA(Phe) by specific metal-ion-promoted cleavages. *Eur. J. Biochem. 182*, 445–450.
(58) Heilman-Miller, S. L., Thirumalai, D., and Woodson, S. A. (2001) Role of counterion condensation in folding of the Tetrahymena ribozyme. I. Equilibrium stabilization by cations. *J. Mol. Biol. 306*, 1157–1166.
(59) Motorin, Y., and Helm, M. (2010) tRNA stabilization by modified nucleotides. *Biochemistry 49*, 4934–4944.
(60) Grilley, D., Misra, V., Caliskan, G., and Draper, D. E. (2007) Importance of partially unfolded conformations for Mg(2+)-induced folding of RNA tertiary structure: structural models and free energies of Mg2+ interactions. *Biochemistry 46*, 10266–10278.
(61) Takamoto, K., He, Q., Morris, S., Chance, M. R., and Brenowitz, M. (2002) Monovalent cations mediate formation of native tertiary structure of the Tetrahymena thermophila ribozyme. *Nat. Struct. Biol. 9*, 928–933.
(62) Perez-Salas, U. A., Rangan, P., Krueger, S., Briber, R. M., Thirumalai, D., and Woodson, S. A. (2004) Compaction of a bacterial group I ribozyme coincides with the assembly of core helices. *Biochemistry 43*, 1746–1753.
(63) Takamoto, K., Das, R., He, Q., Doniach, S., Brenowitz, M., Herschlag, D., and Chance, M. R. (2004) Principles of RNA compaction: insights from the equilibrium folding pathway of the P4-P6 RNA domain in monovalent cations. *J. Mol. Biol. 343*, 1195–1206.
(64) Fang, X., Littrell, K., Yang, X. J., Henderson, S. J., Siefert, S., Thiyagarajan, P., Pan, T., and Sosnick, T. R. (2000) Mg2+-dependent compaction and folding of yeast tRNAPhe and the catalytic domain of the B. subtilis RNase P RNA determined by small-angle X-ray scattering. *Biochemistry 39*, 11107–11113.
(65) Anderson, C. F., Felitsky, D. J., Hong, J., and Record, M. T. (2002) Generalized derivation of an exact relationship linking different coefficients that characterize thermodynamic effects of preferential interactions. *Biophys. Chem. 101−102*, 497–511.
(66) Manning, G. S. (1978) The molecular theory of polyelectrolyte solutions with applications to the electrostatic properties of polynucleotides. *Q. Rev. Biophys. 11*, 179–246.
(67) Record, M. T., Jr., Anderson, C. F., and Lohman, T. M. (1978) Thermodynamic analysis of ion effects on the binding and conformational equilibria of proteins and nucleic acids: the roles of ion association or release, screening, and ion effects on water activity. *Q. Rev. Biophys. 11*, 103–178.
(68) Moghaddam, S., Caliskan, G., Chauhan, S., Hyeon, C., Briber, R. M., Thirumalai, D., and Woodson, S. A. (2009) Metal ion dependence of cooperative collapse transitions in RNA. *J. Mol. Biol. 393*, 753–764.